

DC Accurate Driver for 20-Bit SAR ADC Achieves 2ppm Linearity

Guy Hoover

As resolution and sample rates continue to rise for analog-to-digital converters (ADCs), the driver circuitry for the ADC analog input, not the ADC itself, has increasingly become the limiting factor in determining overall circuit accuracy. First, the driver circuitry must buffer the input signal and provide gain. In addition, it must level shift or convert a single-ended signal to a fully differential signal to satisfy the input voltage range and common mode requirements of the ADC. All must be done without adding distortion to the original signal.

This article presents a simple ADC driver circuit that converts a $\pm 10\text{V}$ single-ended input signal into a fully differential signal capable of driving the LTC2377-20 20-bit SAR ADC with a combined linearity error of only 2ppm. Options for providing higher input impedance and a lower overall supply current are also examined.

CIRCUIT DESCRIPTION

The circuit of Figure 1 converts a $\pm 10\text{V}$ single-ended signal into the $\pm 5\text{V}$ fully differential signal required by the LTC2377-20 (U1). The LTC2377-20 is a 20-bit, 500ksp/s, low power SAR ADC with a typical integral nonlinearity (INL) of $\pm 0.5\text{ppm}$. The voltage at AIN is buffered by U4, which in

turn drives the U5 resistor string, acting as a precision divider. U3 operates in a gain of minus one-half and drives the center of the U5 resistor string to maintain the ADC common mode voltage at $V_{\text{REF}}/2$.

U3 and U4 are LT1468A low offset highly linear op amps. U5 is a LT5400A quad matched resistor network with a guaranteed maximum mismatch of 0.01%. Matched resistor values in U5 are important because any mismatch contributes to both offset and full-scale error in this circuit. For this reason and because of their extremely low voltage coefficient, do not use discrete resistors instead of the LT5400A. R4 provides a quarter-scale shift to the output of U3. R1 and R2 form a divider that biases the noninverting input of U3 at $V_{\text{REF}}/2$.

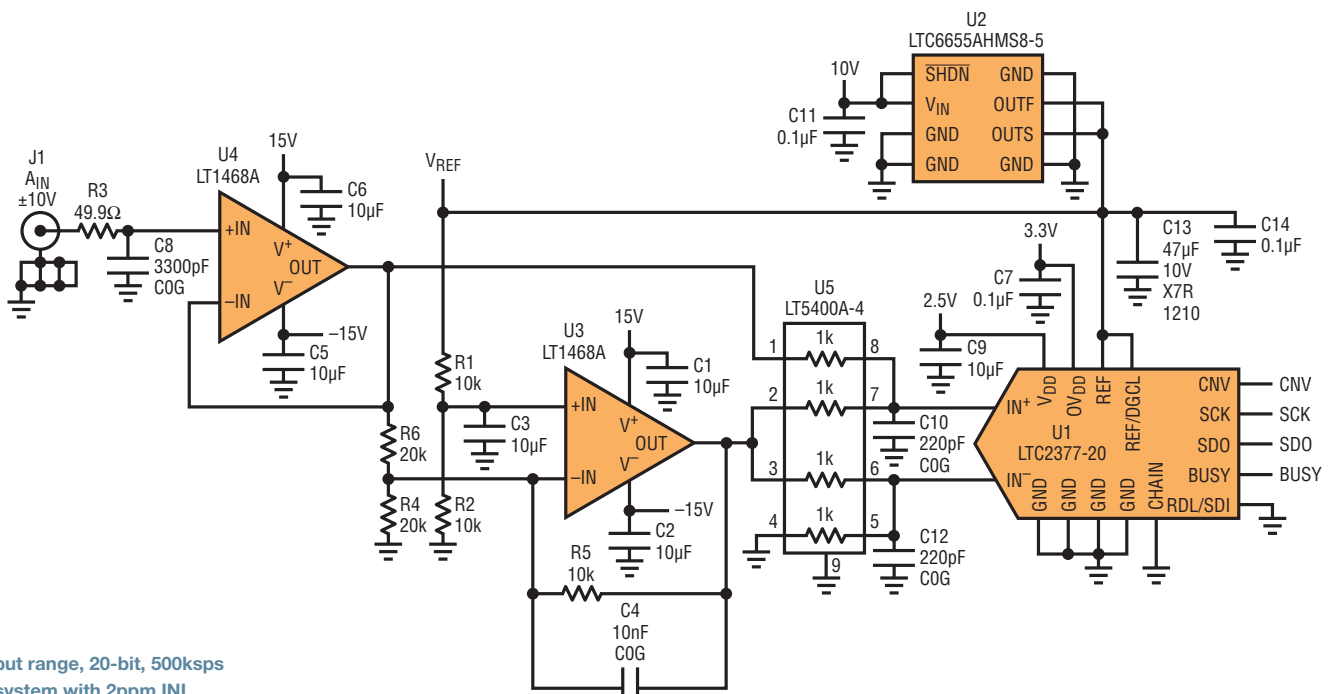


Figure 1. $\pm 10\text{V}$ input range, 20-bit, 500ksp/s data acquisition system with 2ppm INL

The ADC driver circuit shown here converts a single-ended $\pm 10\text{V}$ signal into a $\pm 5\text{V}$ fully differential signal for the LTC2377-20 500ksps SAR ADC. Combined circuit performance achieves $50\mu\text{V}$ offset, 2ppm INL, 102.7dBFS SNR and -123.5dB THD.

R_5 and R_6 set the gain of inverting amplifier U_3 at -0.5 . C_{10} and C_{12} , in combination with the resistors of U_5 , form 1.4MHz filters on the ADC inputs. Additionally, the resistor between pins 1 and 8 of U_5 helps to isolate the output of U_4 from the charge spike that occurs when the ADC goes from hold mode to sample mode. The LTC6655A-5 (U_2) is selected as the reference for this circuit due to its ability to settle quickly from the transients that occur on the REF pin during conversions and because of its low noise.

CIRCUIT PERFORMANCE

Typical AC performance for this circuit includes THD of -123.5dB and SNR of 102.7dBFS at a sample rate of 500ksps with a 100Hz input signal. This performance can be seen in the FFT of Figure 2. The THD and SNR performance are close to the typical numbers found in the LTC2377-20 data sheet, indicating minimal performance degradation when using this driver.

Typical linearity performance for the combined circuit over the entire $\pm 10\text{V}$ input signal range, as shown in Figure 3, is $+2\text{ppm}$, -1.3ppm at a sample rate of 500ksps. Linearity is limited by the INL of the ADC and the CMRR of op amp U_4 .

The combined offset at the ADC input, including the contributions of U_4 , U_5 and U_1 , is measured at $+50\mu\text{V}$. The offset of U_3 has no effect on the offset of this driver. A worst case analysis of offset at the ADC input is calculated by adding the maximum offsets of U_1 , U_4 and U_5 :

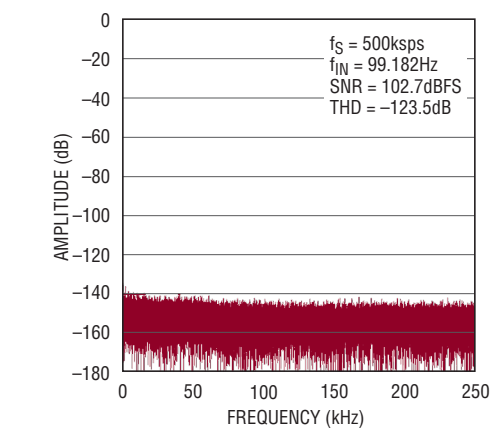


Figure 2. Combined circuit FFT

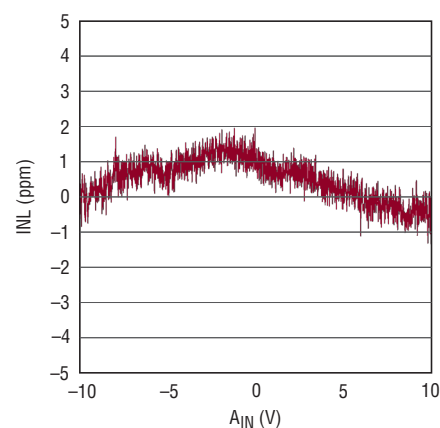


Figure 3. Linearity vs input voltage

$$V_{OS(\text{MAX})} = BZE(\text{MAX})U_1 + \frac{V_{OS(\text{MAX})}U_4}{2} + \left(\frac{V_{REF}}{2} - \frac{V_{REF}}{2 + \frac{\Delta R}{R(\text{MAX})}U_5} \right)$$

$$V_{OS(\text{MAX})} = 13\text{ppm} \cdot 10\mu\text{V/ppm} + 75\mu\text{V}/2 + (5/2 - 5/(2.0001)) \cdot 1\text{E}6\mu\text{V}$$

$$V_{OS(\text{MAX})} = 292\mu\text{V} = 29.2\text{ppm}$$

The LT1468A has a maximum input bias current of $\pm 40\text{nA}$. For applications that require higher input impedance, U_4 can be replaced with the LT1122A. The LT1122A is a fast settling, JFET input op amp with a maximum input bias current of 75pA . Using the LT1122A in this circuit, the INL is $+6\text{ppm}$, -1.1ppm , as shown in the op amp performance comparison in Table 1.

The LTC2377-20 ADC has a typical supply current of 4.2mA at its full sample rate of 500ksps. The LTC2377-20 automatically powers down after a conversion and does not power up until the next conversion is started. This auto power-down feature reduces the power dissipation of the ADC as the sample rate is reduced to as little as $1\mu\text{A}$ for very low sample rate applications.

For low sample rate applications where supply current is important, the 5.2mA maximum supply current of the LT1468A may be too high. The LT1012A picoamp input current, microvolt offset, low noise op amp with a maximum supply current of $500\mu\text{A}$ at

(continued on page 38)

Table 1. Op amp performance comparison

	MAX V_{OS} (μV)	MAX I_B (pA)	TYP I_{SY} (mA)	MAX f_S (ksps)	TYP INL (ppm)
LT1468A	75	40,000	5.2	500	+2, -1.3
LT1122A	600	75	10	500	+6, -1.1
LT1012A	90	150	0.6	125	+0.9, -0.5

The LTC4020 preferentially provides power to the system load and battery charging functions—the system load is always prioritized over charging power—so battery charge current is reduced when necessary during periods of heavy loads. Should the system load exceed the capabilities of the LTC4020 DC/DC converter, battery current will change direction, and load current will be sourced from the battery to supplement the converter output.

the DC/DC converter and battery charger functions when the input is below 35V, so full load current is available whenever the supply is enabled. The SiS862DN switch FETs used here have a typical Q_G of about 10nC each, so with the operating frequency set to 250kHz by resistor R_T , the $Q_{G(TOTAL)} \cdot f_O$ at $V_{IN} = 55V$ falls within the LTC4020's specified $INTV_{CC}$ pass element SOA guidelines.

The IC charges and maintains a 24-cell (48V) lead-acid backup battery using a constant-current/constant-voltage charge profile as previously described. The maximum battery charge current is programmed by R_{CS} to 5A, which is available until the full-charge float voltage of 53.75V is achieved. The battery voltage is monitored by a resistor divider (R_{FB1} and R_{FB2}), which programs the full-charge float voltage of 53.75V (or 2.24V/cell). This divider is referenced through the FBG pin, which is shorted to ground when the LTC4020 is operating, but becomes high impedance when the IC is disabled, reducing the parasitic load on the battery.

The LTC4020 preferentially provides power to the system load and battery charging functions—the system load is always prioritized over charging power—so battery charge current is reduced when necessary during periods of heavy loads. Should the system load exceed the capabilities of the LTC4020 DC/DC converter, battery current will change direction, and load current will be sourced from the battery to supplement the converter output.

When the V_{IN} supply is disconnected, all LTC4020 functions cease and the battery supplies required power to the output. Reverse conduction from the battery through the converter is blocked by the switch FET M4, the battery voltage monitor resistor divider is disconnected via pin FBG, and total battery current into the IC is reduced to less than 10 μ A, maximizing battery life should a no-load storage condition be required.

CONCLUSION

The LTC4020 is a single-IC power management solution for any high power device that requires battery backup or battery-powered remote operation. The integrated buck/boost DC/DC controller can provide power to a voltage rail that is above, below or equivalent to the input voltage. The IC employs an intelligent PowerPath topology, merging the controller output to a full-featured multi-chemistry battery charger. The charger includes an internal onboard timer for charge cycle control and real-time charge cycle monitoring using binary-coded status pins. Three pin-selectable charging profiles provide versatility to accommodate most common battery types with optimized charging characteristics. ■

(LT1468A) continued from page 35)

$\pm 15V$ can replace the LT1468A for these applications. With sample rates up to 125ksps, the LT1012A achieved a linearity of +0.9ppm, -0.5ppm, as shown in the op amp performance comparison in Table 1. At sample rates above 125ksps, the INL performance begins to degrade, as the op amp cannot settle fast enough to accurately drive the ADC.

CONCLUSION

The ADC driver circuit shown here converts a single-ended $\pm 10V$ signal to a $\pm 5V$ fully differential signal for the LTC2377-20 500ksps SAR ADC. Combined circuit performance achieves 50 μ V offset, 2ppm INL, 102.7dBFS SNR and -123.5dB THD. The driver consists primarily of two LT1468A op amps and a LT5400A matched

resistor array. Alternative versions of this circuit use the LT1122A op amp to provide 75pA max input current or the LT1012A op amp at reduced sampling rates to reduce supply current. DC2135, a demo board version of this circuit, is available from Linear Technology. ■